Variability of lightning hazard over Indian region with respect to ENSO Phases

Sreenath Avaronthan Veettil[1], Abhilash Sukumarapillai[1,2], and Vijaykumar Pattathil[1,2]

[1]Department of Atmospheric Sciences, Cochin University of Science and Technology, Cochin 682016, India
[2]Advanced Department Centre for Atmospheric Radar Research, Cochin University of Science and Technology, Cochin 682022, India

Correspondence: Abhilash S (abhimets@gmail.com)

Abstract. The El-Nino Southern Oscillation (ENSO) modulates the lightning flash rate (LFR) variability over India during pre-monsoon, monsoon, and post-monsoon seasons. The impact of ENSO phases on the LFR over the Indian subcontinent is studied using the data obtained from Optical Transient Detector and Lightning Imaging Sensors onboard the TRMM satellite. The study shows that irrespective of ENSO phases, the LFR is maximum over northeast India (NEI) in the pre-monsoon season,

5 and the peak is shifted to the north of northwest India (NNWI) in the monsoon season. The LFR over Northeast India (NEI) and southern peninsular India (SPI) intensified (reduced) during the warm (cold) phase of ENSO in the pre-monsoon season. In the monsoon season, NEI (NNWI) is showing above normal LFR in the warm (cold) ENSO phase. It is fascinating that the three hotspots of LFR over the Indian land region became more prominent in the last decade of the monsoon season. A widespread increase of LFR is observed all over India during the warm phase of ENSO in the post-monsoon season. However,

10 a marked increase in the LFR is confined mostly over the NNWI in the cold ENSO phase. The subtropical westerly jet stream is shifted south in association with the warm phase, and an increase in the geopotential height (GPH) is also noticed all over India in the same period. ENSO's warm phase indirectly influences the LFR over India during the post-monsoon season by pushing the mean position of subtropical westerly towards south latitudes.

1 Introduction

15 Lightning is a tremendous and inescapable atmospheric hazard that humankind has encountered throughout history (Cooray et al., 2007; Mills et al., 2010). For the 14 years from 2001 to 2014, the total number of deaths attributed to lightning hazards are 31725 over India (Selvi and Rajapandian, 2016). The number of casualties underlines lightning hazards as a devastating phenomenon with an annual death rate of 2234 for the above period. Singh and Singh (2015) documented the yearly number of lightning fatalities and lightning flashes in India from 1998 to 2005, and he finds that the fatalities increase coherently with

20 lightning flash rate. Lightning strikes over the plain terrain are observed to less as compared to the hilly regions. Due to the high population density of the former, even lesser lightning flashes take many people's lives due to high chances of being struck by lightning (Yadava et al., 2020).

The El-Nino Southern Oscillation (ENSO) is a naturally occurring planetary-scale phenomenon related to the variations in sea surface temperatures over the tropical Pacific Ocean, strongly influencing the number of flashes and average flash rate

25 (Kumar and Kamra, 2012). It is one of the most dynamic climatic variability modes, characterized by three phases: El-Nino (Warm), La-Nina (Cold), and Neutral. The ENSO is a crucial player in the transport of heat, moisture, and momentum and modulates the frequency, intensity, and location of deep convection and the associated lightning activity (Williams, 1992; Kulkarni and Siingh, 2014). Higher Lightning Flash Rate (LFR) areas are located away from the equator during the warm phase and coincide with regions of anomalous jet stream circulation enhanced by the meridional heat transport (Chronis et al.,

30 2008). Kandalgaonkar et al. (2010) has reported that lightning activity during the El-Nino year of 2002 increased by 18% over the Indian land region compared to the La-Nina years during 1998-2011. On a global scale, lightning activity shows strong regional preference during different ENSO Phases.

The changes in the lower and upper air circulations associated with different ENSO phases have been found to influence the storm frequency and intensity (Yang et al., 2002; Hsu and Wallace, 1976), which in turn affect the lightning activity

35 (Goodman et al., 2000). Kent et al. (1995) observed that ENSO could dictate the distribution of clouds over the tropics and subtropics. Owing to the presence of anomalous subsidence over the western Pacific and adjacent landmass, deep convective clouds are inhibited; hence the rainfall is less during the warm phase (Cess et al., 2001). A southward/eastward shift in the global lightning activity is visible during the warm phase, and the latitudes corresponding to the descending limb of the Hadley circulation exhibit the most significant contrast of LFR between the warm and cold phase of the ENSO (Sátori et al., 2009).

40 Generally, lightning activity is controlled by the clouds growing deep into the atmosphere. The deep convective cores present over the east coast of India during the pre-monsoon season shift to the foothills of western Himalayas during the monsoon (Romatschke et al., 2010). Cecil et al. (2014) documented that the offshore regions of India and the maritime continent are prone to deep convection. The vertical growth of cloud systems is amplified by the intense updraft, promoting ice crystals and supercooled liquid (mixed-phase) inside the convective system. The interaction between these hydrometeors is mainly

45 responsible for the electrification inside the cloud (Takahashi et al., 1999; Williams, 2001). Topography plays a critical role in the development of deep convective clouds and impacts the distribution of lightning activity (Kilinc and Beringer, 2007). Earlier studies have observed that elevated landmass favors the development of deep convective clouds (Zipser et al., 2006; Houze Jr et al., 2007; Rasmussen and Houze Jr, 2011) and thereby leading to higher LFR. The dynamic and thermodynamic states of the atmosphere also modulate the lightning activity over a region (Williams, 1992; Zipser, 1994; Petersen et al., 1996; Rosenfeld,

50 1999). Another agent that plays a decisive role in generating lightning activity is aerosols. Higher aerosol loading increases the available liquid water in the mixed-phase condition, which is an essential factor for cloud electrification and lightning activity (Williams et al., 2002). Venevsky (2014) reported a significant correlation between lightning and concentration of annually-averaged cloud condensation nuclei over both land and ocean.

The awareness of lightning safety among the public is relatively low. The present study provides vital information on the risky

55 lightning periods over the Indian subcontinent and how the large scale phenomenon, ENSO, is influencing the same. We are detailing the modulation of LFR under different ENSO phases with the help of a vertical profile of hydrometeors (graupel and snow) inside the cloud systems and related atmospheric dynamics during pre-monsoon, monsoon, and post-monsoon seasons in India. The variability of LFR and hydrometeor distribution inside the convective system with different ENSO phases is very rare in the literature.

2 Data and methods

The Lightning Imaging Sensor (LIS) was an instrument onboard the Tropical Rainfall Measuring Mission (TRMM) satellite launched in December 1997. This instrument senses lightning flashes across the global tropics and subtropics (Goodman et al., 2007). The Optical Transient Detector (OTD) was the predecessor of LIS, launched in the MicroLab-1 satellite in April 1995. The LIS/OTD data product from July 1995 to December 2013 gives the LFR at a spatial resolution of 2.5° × 2.5° and a temporal resolution of 1 day. The TRMM-3A12 data provide the distribution of hydrometeors (graupel, snow, rainwater) inside the convective systems. The monthly averaged vertical profiles of hydrometeors, and latent heat used in this study are from above data set. The data set is having a spatial resolution of 0.5° × 0.5°, and it available from January 1998 to December 2013. It has 28 vertical levels, which start from 0.5 km, and each level is separated by 0.5 km. The modulation of Geopotential height (GPH) at 500 hPa, wind at 200 hPa, and specific humidity (SH) at 300 hPa are also examined with the ENSO phases from July 1995 to December 2013. The above parameters are obtained from the NCEP-NCAR reanalysis data with a similar spatial and temporal resolution of LFR. Oceanic Nino Index (ONI) is the standard used to identify different phases of ENSO. The average value of ONI is determined during pre-monsoon, monsoon, and post-monsoon season by using Hadi SST data and detailed in table 1. If ONI value is above +0.5° (-0.5°) C, it is taken as the warm (cold) phase, and the neutral phase corresponds to the ONI index lies between -0.5/+0.5° C .

3 Results and discussion

3.1 Composite LFR with respect to ENSO phases

Figure 1 represents the LFR composites for pre-monsoon, monsoon, and post-monsoon seasons corresponding to the three ENSO phases. Irrespective of ENSO phases, the LFR peak is located over northeast India (NEI) during the pre-monsoon season while its peak shifts to the north of northwest India (NNWI) in the monsoon season. Kamra and Athira (2016) have previously reported a similar type of swing in LFR between pre-monsoon and monsoon seasons. The Himalayan orography favours the formation of deep convective systems over the NEI (Goswami et al., 2010) and is evidenced by the high values of LFR over the region. Rather than the altitude, the steep topographic gradient is responsible for producing deep convection. The deep convective clouds developed in the conditionally unstable atmosphere during the pre-monsoon season are electrically more active (Williams et al., 1992). Lau et al. (2008) proposed that during the pre-monsoon months, dust and black carbon from neighbouring sources accumulates over the Indo-Gangetic plain against the foothills of Himalayas and act as an elevated heat pump (EHP). The enhanced warming in the middle and upper troposphere contributes to the genesis of deep clouds and higher LFR.

Compared to monsoon and post-monsoon seasons, convective available potential energy (CAPE) is higher during the pre-monsoon season. The maximum values appear over the southern peninsular region and the east coast of India, and the average value is above 1500 J/kg all over India (Murugavel et al., 2014). The regions of higher values of LFR (Figure 1) during the pre-monsoon season coincide with the regions of CAPE maxima reported by (Murugavel et al., 2014). The moderate updrafts

Year	Pre-monsoon	Monsoon	Post-monsoon
1995	0.39	-0.08	*-0.60*
1996	-0.27	-0.10	-0.25
1997	**0.51**	**1.81**	**2.41**
1998	**1.15**	*-0.57*	*-1.20*
1999	*-0.73*	*-0.77*	*-1.24*
2000	*-0.80*	-0.39	*-0.65*
2001	-0.22	0.01	-0.25
2002	0.27	**0.81**	**1.40**
2003	0.10	0.15	0.46
2004	0.14	**0.58**	**0.76**
2005	0.41	0.14	-0.36
2006	-0.27	0.39	**1.02**
2007	*-0.10*	-0.40	*-1.40*
2008	*-0.76*	-0.08	-0.43
2009	-0.35	**0.73**	**1.49**
2010	**0.62**	*-0.97*	*-1.52*
2011	*-0.61*	-0.34	*-0.96*
2012	-0.17	**0.53**	0.21
2013	-0.03	0.39	**0.79**

Table 1. ONI during the pre-monsoon, monsoon, and post-monsoon season in India from 1995 to 2013. The bold, italics and underlined values denote El-Nino, La-Nina, and Neutral phases of ENSO, respectively.

limit the vertical development of convective clouds during the summer monsoon under the influence of maritime air mass (Kumar et al., 2014; Tinmaker et al., 2015), which leads to a decline in the cloud electrification during the monsoon season. Among the three seasons, post-monsoon shows a minimum of LFR over the Indian region (Figure 1), and the NW to the NE gradient of LFR is also observed to be weak in this season. The average value of CAPE during the season is less than 500 J/kg over most parts of India (Murugavel et al., 2014), which is quite low to favour the development of deep convection and hence lightning.

3.2 Distribution of LFR during pre-monsoon season with respect to ENSO phases

There are three hot spots of high lightning activity over the Indian subcontinent (Figure 1). They are located in the NEI (85°E-95°E, 20°N-30°N), NNWI (25°N-40°N, 65°E-80°E), and southern peninsular India (SPI) (5°N-15°N, 75°E-80°E). We have examined the variability of the hydrometeors inside the convective systems that develop over these regions to understand their association with LFR. The LFR values are low during the pre-monsoon season over NNWI when the ENSO phase is either warm or cold (Figure 2 (a, b)). However, the same region exhibits an increase of LFR during the normal phase (Figure 2 (c)).
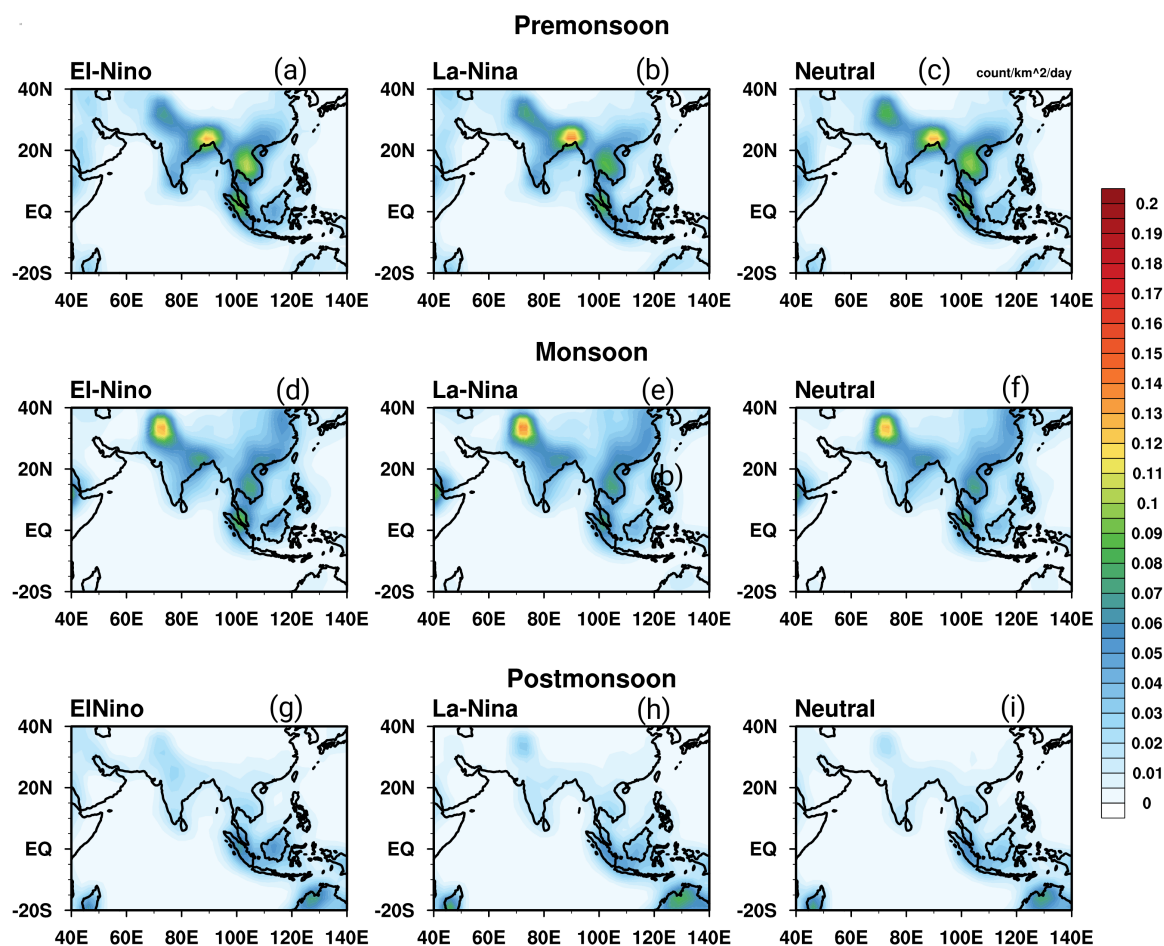
Figure 1. LFR composite during different ENSO phases.

While looking into the LFR anomaly of individual years, three years (1997, 1998, and 2010) of pre-monsoon have come under
the El-Nino phase. The first two exhibits a decrease of LFR over NNWI, which contributes to the overall reduction in the LFR.
Out of the four La-Nina years (1999, 2000, 2008, and 2011) of pre-monsoon season, 1999, 2000, and 2011 have below-average
values of LFR over the same region (Figure 3 (d)). The pre-monsoons of 11 years occurred during the normal phase of ENSO,
in which six years are showing below, and five years above-average values of LFR over NNWI.

The amount of graupel and snow content decreased over NNWI during the warm and cold phase of ENSO (Figures 4 (d),
5 (d)), which in turn decrease the LH release (Figure 6 (d)). The negative anomaly of SH at 300 hPa manifests that the clouds
are unbaled to penetrate deep into the atmosphere during these two phases over NNWI (Figure 7 (a, b)). As a result, LFR over
NNWI in these phases is low, especially in the cold phase. The higher value of LFR during the normal phase is due to the
abundance of graupel and snow inside the cloud system. The ENSO warm phase during the pre-monsoon season is favourable
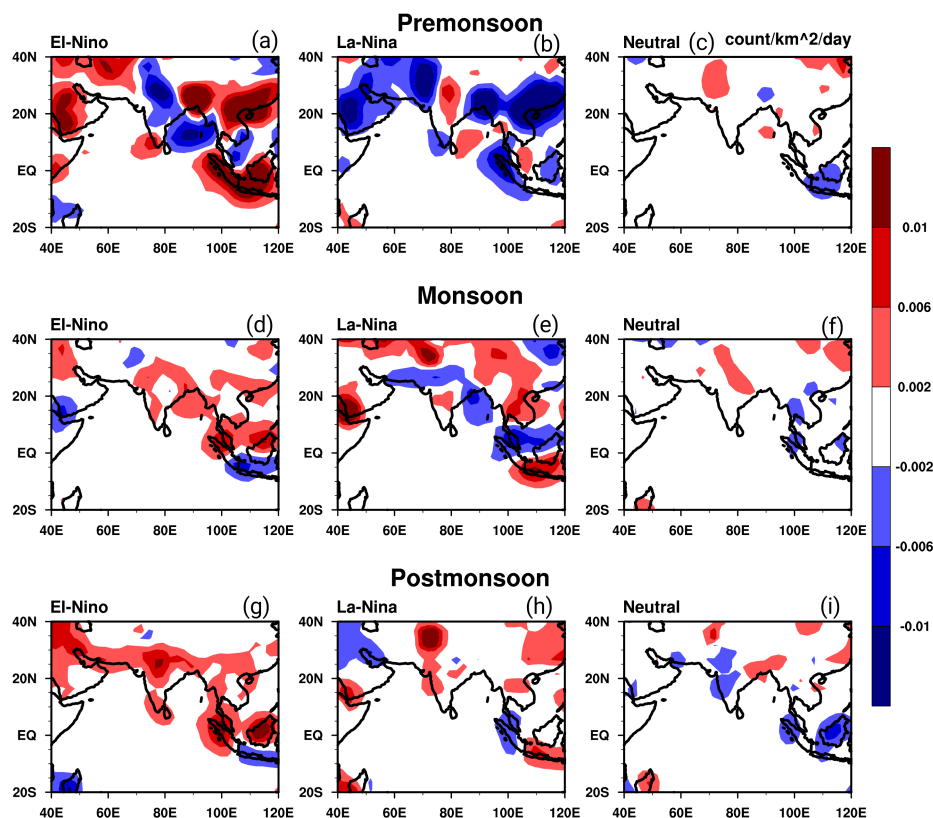
Figure 2. Anomaly composite of LFR during different ENSO phases.

to LFR over the NEI and SPI but unfavourable to central India (CI) (Figure 2 (a)). On the contrary, the cold ENSO phase

115 suppresses LFR over NEI and SPI with enhanced LFR over CI (Figure 2 (b)). In short, the anomaly pattern of LFR during

warm and cold phases are mirror images of each other during the pre-monsoon season. Most of the regions that exhibit an

increase of LFR in the warm period show decreased LFR in the cold phase of ENSO. The entire years under the cold (warm)

phase during pre-monsoon are showing a decrease (increase) of LFR over NEI (SPI) (Figure 3 (a, g)), which firmly indicates

that the cold phase suppresses the LFR over NEI, and the warm phase enhance it over SPI. The vertical profile of graupel

120 shown in figure 4 (a) indicates that clouds over NEI have high (low) graupel content during the ENSO warm (cold) phase. An

increase of snow content with a peak value near 6.5 km is also observed over NEI during pre-monsoon (Figure 5 (a)). The

interaction between snow and graupel and the associated charge generation is responsible for the occurrence of lightning in

convective clouds. The formation of the higher (lower) amount of graupel and snow over NEI during the warm (cold) phase

will release more latent heat, which is evident from figure 6 (a). The above (below) normal value of SH over NEI indicates

125 that the convective clouds formed during the ENSO warm (cold) phase are vigorous (wimpy) and which is responsible for the

enhanced (reduced) LFR. Figures 4 (g) and 5 (g) show that the graupel and snow concentrations over SPI are anomalously

high up to 6 km during the cold phase of ENSO; and above that level, it decreases. The pattern of such hydrometeors reverses during the warm phase and exhibits below-average values beneath 6 km and rapidly increases above that level. The level of maximum latent heat release follows the pattern of graupel and snow concentrations (Figure 6 (g)). These results confirm that

130 the warm phase of ENSO intensifies the deep convection over SPI during pre-monsoon season and hence promote LFR.
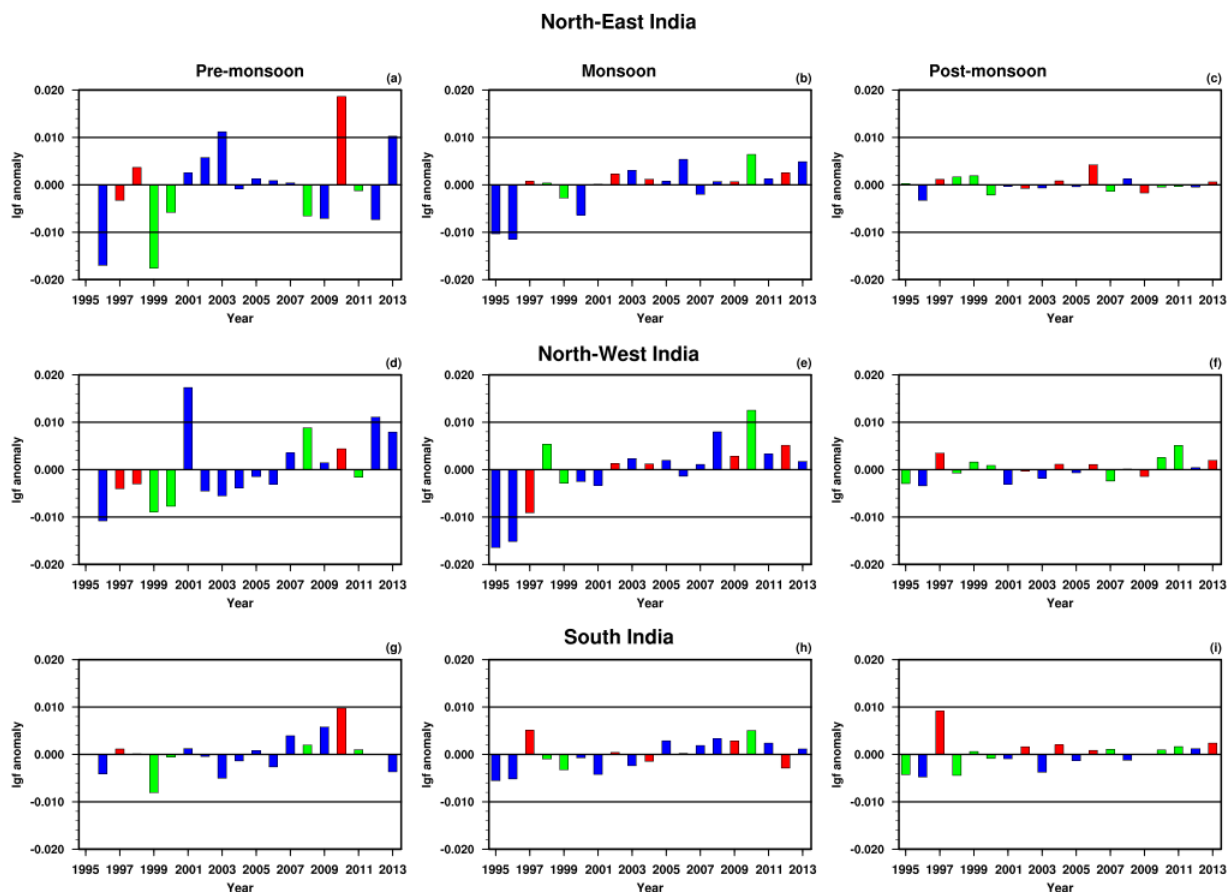
Figure 3. The anomaly of LFR during the individual years with different ENSO phases. Red color label bar corresponds to warm; green one corresponds to the cold and blue color label bar indicates the neutral phases of ENSO

3.3 Distribution of LFR during monsoon season with respect to ENSO phases

The LFR over the monsoon trough region and along the northwest coast of India increases during the warm phase of ENSO (Figure 2 (d)) but remarkably decreases during the cold phase (Figure 2 (e)). Based on the 1998-1999 El-Nino event, Hamid
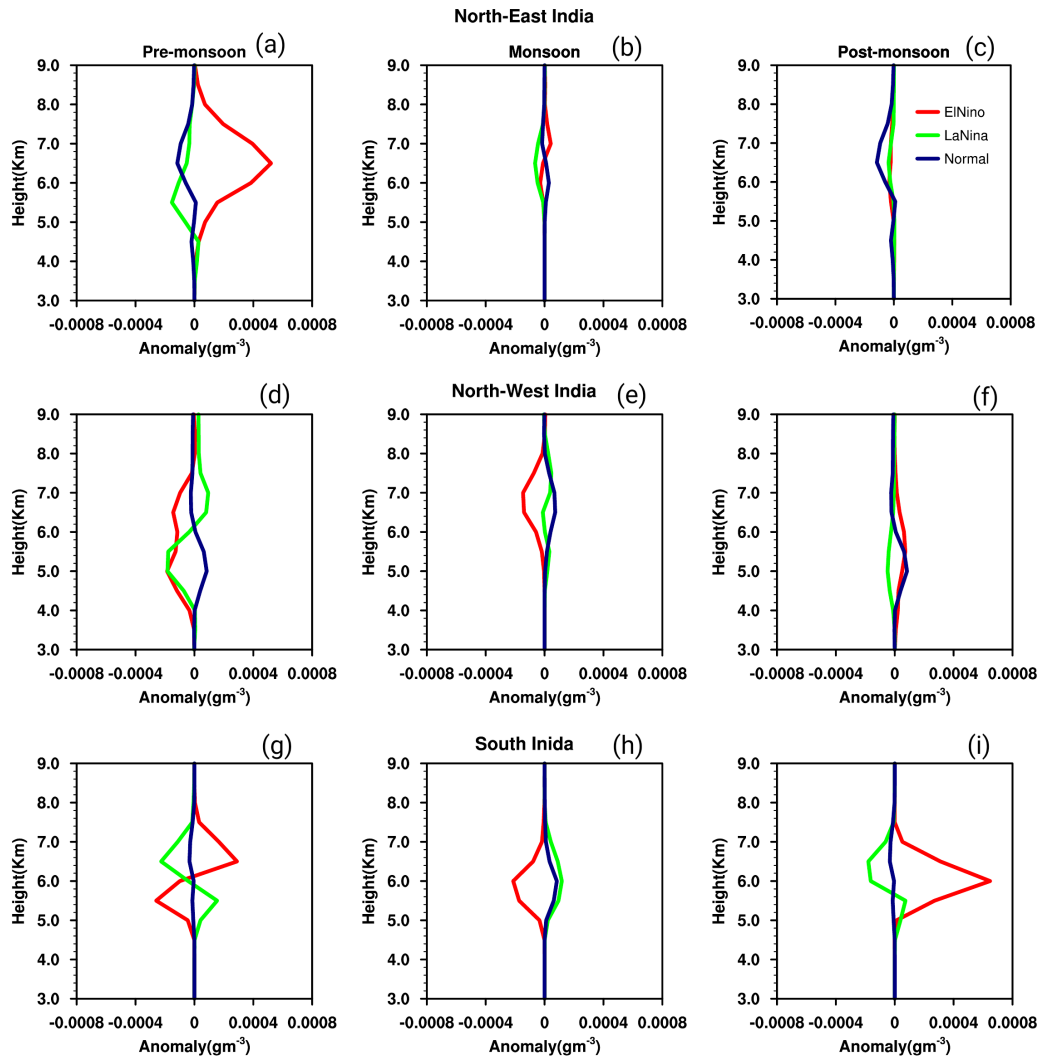
Figure 4. Anomaly composite of groupel during different ENSO phases.

et al. (2001) suggested that intense convective storms developing over the maritime continents are responsible for the increase
of lightning activity despite a decrease in the number of convective storms. During the El-Nino years of 1997-1998 and 2002-
2003, the southeast Asian regime exhibited an above-average value of lightning (Kumar and Kamra, 2012). An elongated
region, over central India, is showing higher (lower) LFR during the warm (cold) phase of ENSO (Figure 2 (d, e)). While
analysing the 300 hPa SH variability, we noticed that the amount of SH over that region is high during the warm and low
during the cold phase (Figure 7 (d, e)). The NEI is showing positive anomaly of LFR during both warm and cold phases of
ENSO. Figure 3 (b) enforces this result by indicating that all the years under the warm phase and the majority of years under the

cold phase (during the monsoon season) show an increase in LFR over NEI. The similarity in the LFR anomaly is noticeable in

the distribution of graupel and snow during the two phases (Figure 4 (b), 5 (b)). In contrast, the LFR is enhanced (suppressed)

over NNWI during the cold (warm) period due to the presence of a larger (smaller) amount of graupel and snow. There is no

noticeable change in the distribution of LFR over SPI in the three phases of ENSO (Figure 2 (d, e, f). Anomaly pattern of LFR

145   in individual years is not exhibiting any particular pattern corresponding to different ENSO phases over SPI (Figure 3 (h)).
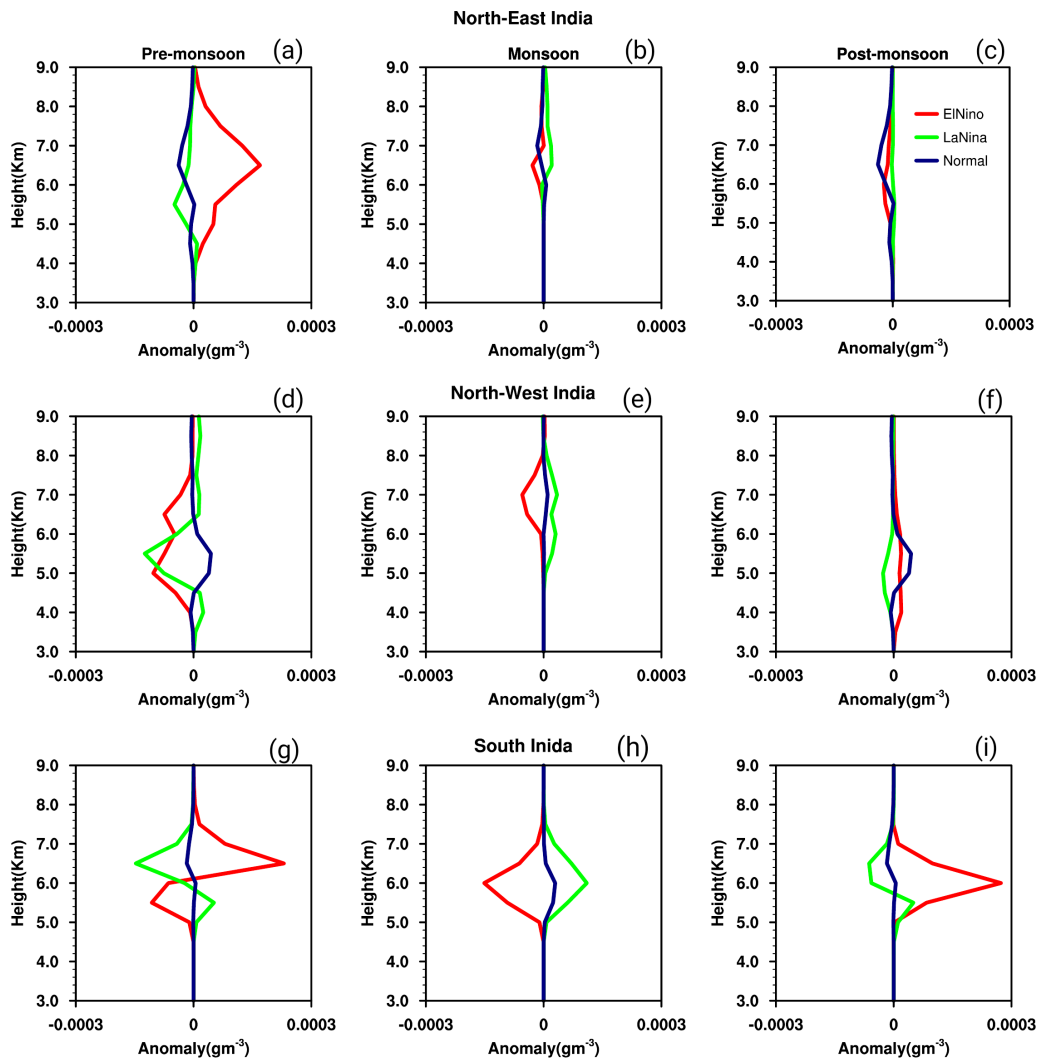
Figure 5. Composite anomaly of snow during different ENSO phases.

It is interesting that during the 12 years from 2002 to 2013, 11 years have shown above-average values of LFR over the NEI

and NNWI regions (Figure 3 (b, e)), demonstrating the intensification of deep convective cloud formation during the recent
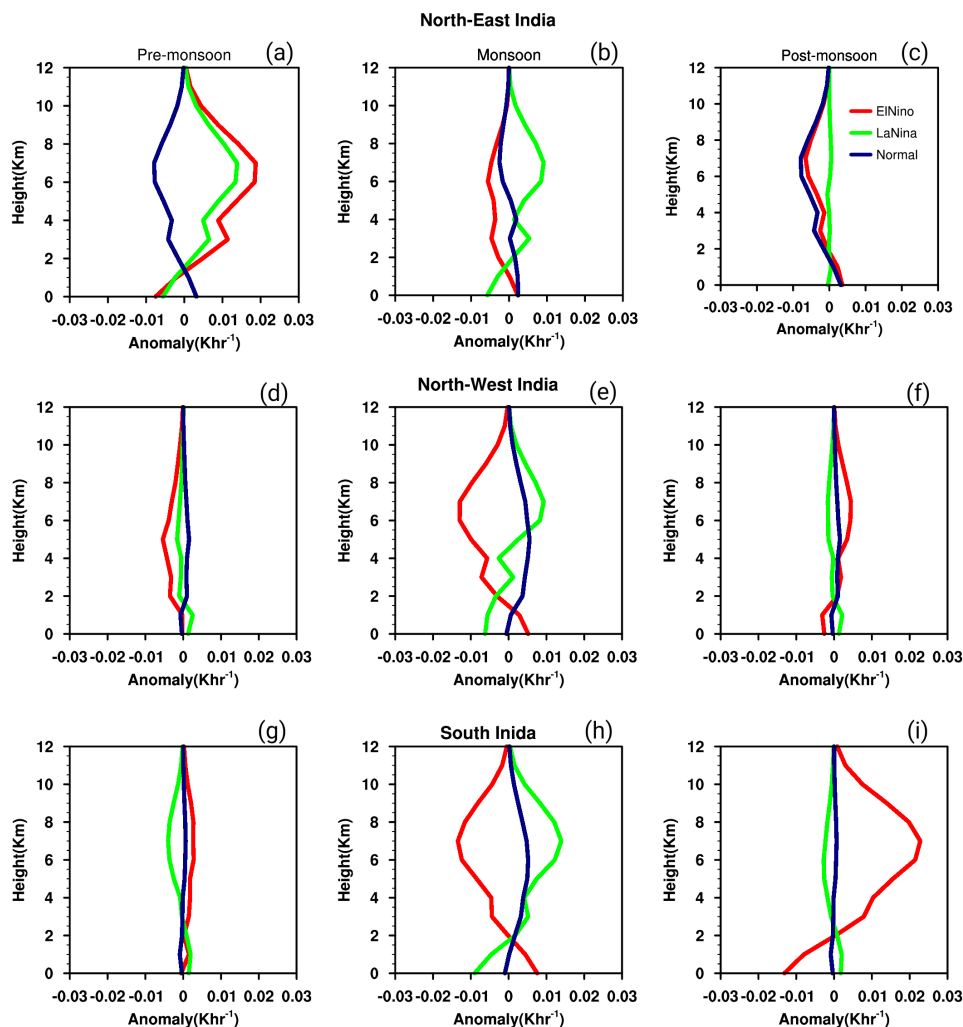
Figure 6. Composite anomaly of latent heat during different ENSO phases.

monsoon season over respective areas. Out of the nine years from 2005 to 2013, 8 have above-normal LFR over SPI (Figure 3
(h)). This indicates an escalation of deep convection over SPI in that period. In other words, during monsoon season, the three
150 hotspots of LFR over the Indian land region became more prominent in the last decade.

3.4 Distribution of LFR during post-monsoon season with respect to ENSO phases

During the post-monsoon season, the Western disturbances (WD), which are vertical perturbations associated with the subtrop-
ical westerly jet stream, bring rainfall to India's northern regions (Dimri et al., 2016). The jet is more intense and propagates
southward during the El-Nino phase of ENSO (Schiemann et al., 2009). The post-monsoon El-Nino period shows an increase
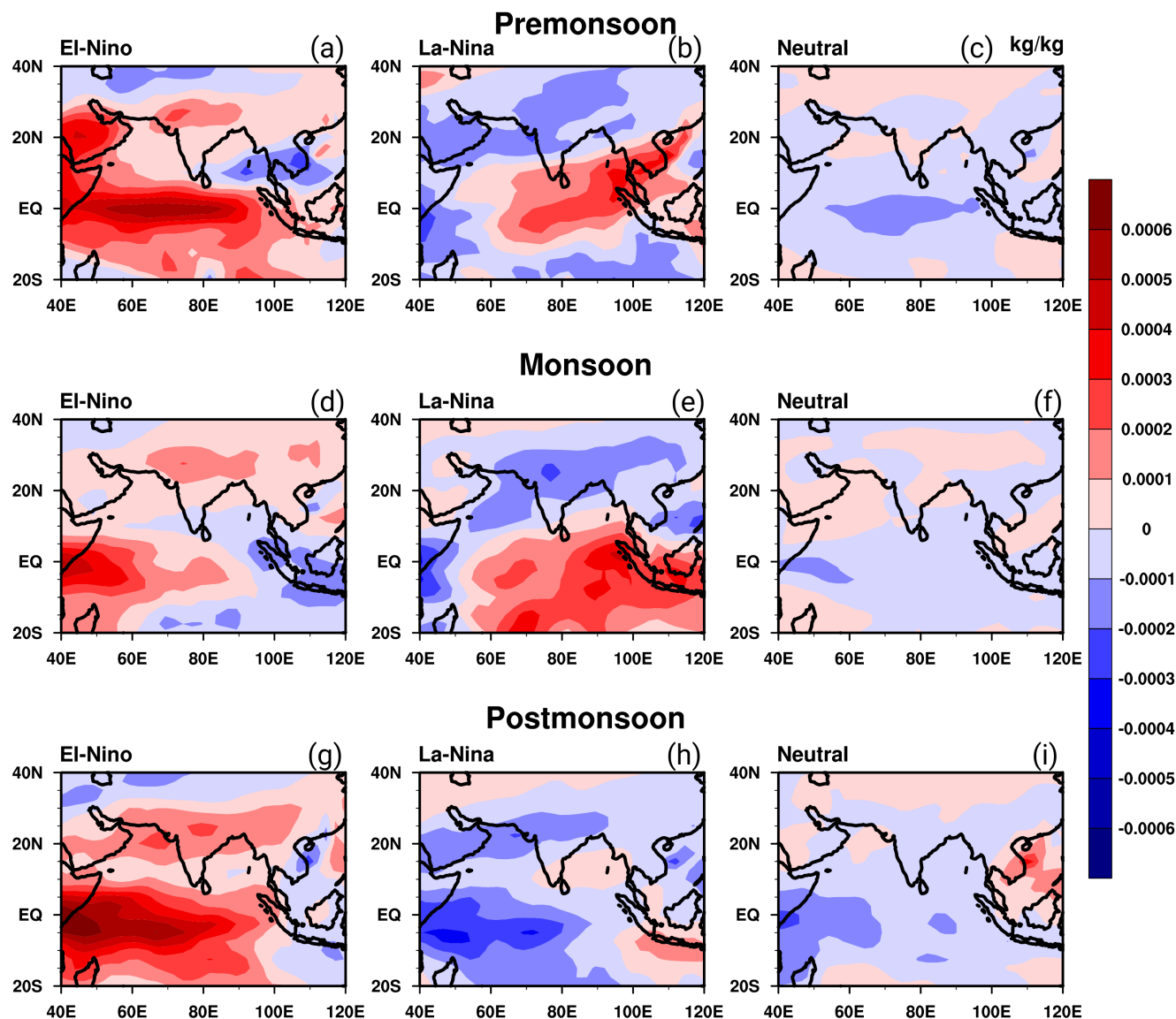
Figure 7. Anomaly composite of specific humidity at 300hPa during different ENSO phases.

155 of LFR throughout the country, and it is maximum over north-central India (Figure 2 (g)). In contrast, in the cold phase, intense
LFR is concentrated only over the NNWI (Figure 2 (h)). The NEI and NNWI are not showing any significant difference in the
vertical profile of snow and graupel with different ENSO phases during the post-monsoon season (Figures 4 (c, f) and 5 (c, f)).
Zubair and Ropelewski (2006) reported that there exists a significant role for ENSO on controlling the post-monsoon rainfall
over SPI. The SPI is showing an increase of LFR in the warm phase of ENSO during the season due to the presence of clouds
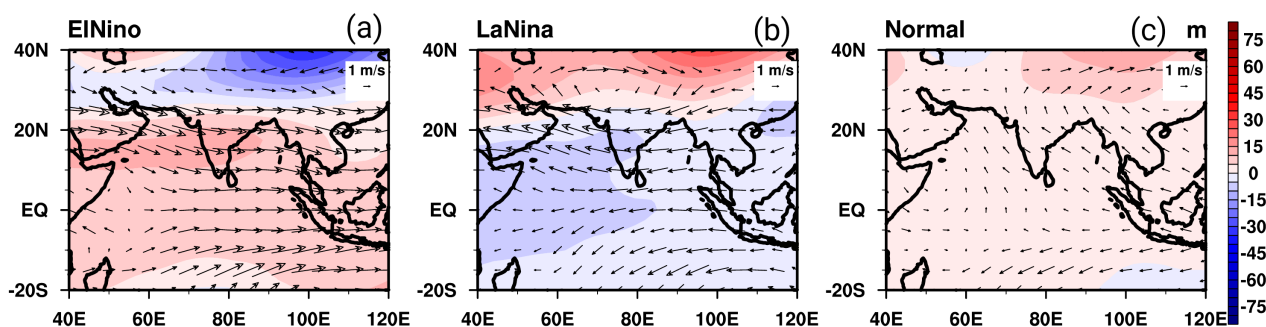
Figure 8. Anomaly composite of geopotential height at 500hPa and 200hpa wind during different ENSO phases.

160 having higher graupel and snow content over that region (Figures 2 (g), 4 (i), 5 (i)). The entire years grouped under the warm phase of ENSO during the post-monsoon season show an increase of LFR over SPI. On the other hand, in the years of the cold phase, the LFR anomaly pattern is not uniform (Figure 3 (i)). Climate variability, like ENSO, can alter the position of jet streams and hence the distribution of WD (Hunt et al., 2018). Syed et al. (2006) identified that the intensification of WDs during the El-Nino is associated with the weakening of Siberian high. The depressions formed over the South Bay of Bengal, and
165 the Arabian Sea can also modulate WDs' path (Rao et al., 1969). The 500 hPa GP surface drops-down (go up) from the 25°N towards the north and indicates the suppression (enhancement) of convection over that region during the warm (cold) phase of ENSO (Figure 8 (a, b)). In contrast, a higher (lower) GP surface is visible all over India during the warm (cold) phase, which is an indication of an increase (decrease) in the convective activity during the respective phases. By considering the anomalous circulation at 200 hPa level, an anomalous westerly (easterly) wind is prevalent over entire India during warm (cold) periods
170 (Figure 8 (a, b)). The upper-level wind pattern and variability in the GPH together indicate the southward extension of WD during ENSO's warm phase. The sharp increase (decrease) of SH lies precisely over the region of the maximum undulation of GPH during the warm (cold) phase (Figure 7 (g, h)). This suggests that ENSO indirectly influences the LFR over India during the post-monsoon season by modulating WDs' path.

4 Conclusion

175 In this study, we have discussed the influence of ENSO on LFR during pre-monsoon, monsoon, and post-monsoon seasons over India. Regardless of ENSO phases, the LFR is peaking at the time of pre-monsoon season over NEI and SPI. However, the NNWI exhibits a peak LFR during the monsoon season. The LFR is increased (decreased) over NEI and SPI during the warm (cold) phase of ENSO, and anomalies of the charge generating hydrometeors show a similar kind of swing. The entire years under the cold (warm) phase during the pre-monsoon season taken in this study is characterized by a decrease (increase)
180 of LFR over NEI (SPI), which firmly indicates that the cold phase suppresses the LFR over NEI, and the warm phase enhance it over SPI.

During the cold phase in pre-monsoon, the graupel and snow concentration over SPI shows an above-average value up to 6 km. The pattern of these hydrometeors reverses during the warm phase. The increase in graupel and snow formation above 6 km, pinpoint that the warm phase of ENSO is conducive for deep convection over SPI during the pre-monsoon and hence high LFR. The neutral phase of ENSO favours deepening of clouds over NNWI, as evidenced by the high values of the upper level-specific humidity. At the time of monsoon season, the LFR over NEI is high during both El-Nino and La-Nina periods. Over NNWI, LFR increases during La-Nina but diminishes during El-Nino. The SPI does not show significant variation in LFR with respect to different ENSO phases during the monsoon season. While considering the recent 12 years of this study, irrespective of the ENSO phases, every year has displayed above-average values of LFR over the NEI and NNWI region. Out of 9 years from 2005 to 2013, 8 displayed above-normal LFR over SPI, signifies the intensification of LFR over the three hotspots in the last decades of the monsoon season. Almost all regions in India are exhibiting higher LFR during the warm ENSO phase in the post-monsoon season. The elevated (reduced) GPH is visible all over India during the warm (cold) phase of ENSO, which is an indication of an increase (decrease) in the convective activity during the respective phases. The entire years grouped under the warm phase of ENSO during the post-monsoon season show an increase of LFR over SPI, whereas the years elected under the cold phase shows disperse in the anomaly pattern. Both intensification and southward extension of WD is responsible for higher LFR over India in the warm phase, an indication of indirect interaction between ENSO and LFR by modulating the mid-latitude westerlies.

Data availability. The LIS/OTD data and vertical profiles of hydrometeors, and latent heat obtained from the website http://ghrc.nsstc.nasa.gov/ and https://disc.gsfc.nasa.gov/datasets/ respectively. The GPH, wind and SH data are avilable the weblink https://psl.noaa.gov/data/gridded/ data.ncep.reanalysis.html. The HadISST data used in this work is accessible from the weblink https://psl.noaa.gov/gcos$_w$gsp/.

Author contributions. The paper and its methodology were conceptualized and developed by AS, SAV, and VP; SAV performed the analyses, and VP curated the data. The original draft preparation was by SAV; further reviewingand editing was by VP and AS. SAV handled visualization.

Competing interests. The authors declare that they have no known competing financial interests or personal relationships that could have appeared to influence the work reported in this paper.

Acknowledgements. We are grateful to NASA and PSL for providing LIS/ODT, TRMM, and NCEP Reanalysis data products, respectively, which are used in this study. Sreenath A V acknowledges Kerala State Council for Science, Technology, and Environment (KSCSTE), India, for providing financial support. Support from the Department of Atmospheric Sciences, Cochin University of Science and Technology is acknowledged.

References

Cecil, D. J., Buechler, D. E., and Blakeslee, R. J.: Gridded lightning climatology from TRMM-LIS and OTD: Dataset description, Atmospheric Research, 135, 404–414, 2014.

Cess, R. D., Zhang, M., Wielicki, B. A., Young, D. F., Zhou, X.-L., and Nikitenko, Y.: The influence of the 1998 El Niño upon cloud-radiative forcing over the Pacific warm pool, Journal of climate, 14, 2129–2137, 2001.

Chronis, T., Goodman, S., Cecil, D., Buechler, D., Robertson, F., Pittman, J., and Blakeslee, R.: Global lightning activity from the ENSO perspective, Geophysical Research Letters, 35, 2008.

Cooray, V., Rakov, V., and Theethayi, N.: The lightning striking distance—Revisited, Journal of Electrostatics, 65, 296–306, 2007.

Dimri, A., Yasunari, T., Kotlia, B., Mohanty, U., and Sikka, D.: Indian winter monsoon: Present and past, Earth-science reviews, 163, 297–322, 2016.

Goodman, S., Buechler, D., Knupp, K., Driscoll, K., and McCaul Jr, E.: The 1997–98 El Nino event and related wintertime lightning variations in the southeastern United States, Geophysical Research Letters, 27, 541–544, 2000.

Goodman, S., Buechler, D., and McCaul, E.: Lightning, in Our Changing Planet: The View From Space, 44–52, 2007.

Goswami, B. B., Mukhopadhyay, P., Mahanta, R., and Goswami, B.: Multiscale interaction with topography and extreme rainfall events in the northeast Indian region, Journal of Geophysical Research: Atmospheres, 115, 2010.

Hamid, E. Y., Kawasaki, Z.-I., and Mardiana, R.: Impact of the 1997–98 El Niño event on lightning activity over Indonesia, Geophysical Research Letters, 28, 147–150, 2001.

Houze Jr, R. A., Wilton, D. C., and Smull, B. F.: Monsoon convection in the Himalayan region as seen by the TRMM Precipitation Radar, Quarterly Journal of the Royal Meteorological Society: A journal of the atmospheric sciences, applied meteorology and physical oceanography, 133, 1389–1411, 2007.

Hsu, C.-P. F. and Wallace, J. M.: The global distribution of the annual and semiannual cycles in precipitation, Monthly Weather Review, 104, 1093–1101, 1976.

Hunt, K. M., Turner, A. G., and Shaffrey, L. C.: The evolution, seasonality and impacts of western disturbances, Quarterly Journal of the Royal Meteorological Society, 144, 278–290, 2018.

Kamra, A. and Athira, U.: Evolution of the impacts of the 2009–10 El Niño and the 2010–11 La Niña on flash rate in wet and dry environments in the Himalayan range, Atmospheric Research, 182, 189–199, 2016.

Kandalgaonkar, S., Kulkarni, J., Tinmaker, M., and Kulkarni, M.: Land-ocean contrasts in lightning activity over the Indian region, International Journal of Climatology: A Journal of the Royal Meteorological Society, 30, 137–145, 2010.

Kent, G., Williams, E., Wang, P., McCormick, M., and Skeens, K.: Surface temperature related variations in tropical cirrus cloud as measured by SAGE II, Journal of Climate, 8, 2577–2594, 1995.

Kilinc, M. and Beringer, J.: The spatial and temporal distribution of lightning strikes and their relationship with vegetation type, elevation, and fire scars in the Northern Territory, Journal of climate, 20, 1161–1173, 2007.

Kulkarni, M. and Siingh, D.: The relation between lightning and cosmic rays during ENSO with and without IOD—a statistical study, Atmospheric Research, 143, 129–141, 2014.

Kumar, P. R. and Kamra, A.: Variability of lightning activity in South/Southeast Asia during 1997–98 and 2002–03 El Nino/La Nina events, Atmospheric research, 118, 84–102, 2012.

Kumar, S., Hazra, A., and Goswami, B.: Role of interaction between dynamics, thermodynamics and cloud microphysics on summer monsoon precipitating clouds over the Myanmar Coast and the Western Ghats, Climate dynamics, 43, 911–924, 2014.

245 Lau, K.-M., Ramanathan, V., Wu, G.-X., Li, Z., Tsay, S., Hsu, C., Sikka, R., Holben, B., Lu, D., Tartari, G., et al.: The Joint Aerosol–Monsoon Experiment: A new challenge for monsoon climate research, Bulletin of the American Meteorological Society, 89, 369–384, 2008.

Mills, B., Unrau, D., Pentelow, L., and Spring, K.: Assessment of lightning-related damage and disruption in Canada, Natural hazards, 52, 481–499, 2010.

Murugavel, P., Pawar, S., and Gopalakrishan, V.: Climatology of lightning over Indian region and its relationship with convective available

250 potential energy, International Journal of Climatology, 34, 3179–3187, 2014.

Petersen, W. A., Rutledge, S. A., and Orville, R. E.: Cloud-to-ground lightning observations from TOGA COARE: Selected results and lightning location algorithms, Monthly weather review, 124, 602–620, 1996.

Rao, Y., Srinivasan, V., Raman, S., and RAMAKRISHNAN, A.: Forecasting manual, Part-II, Discussion of typical synoptic weather situation, winter-western disturbances and their associated features. FMU Report No. III-1.1, India Meteorological Department. Delhi, India, 1969.

255 Rasmussen, K. L. and Houze Jr, R. A.: Orogenic convection in subtropical South America as seen by the TRMM satellite, Monthly Weather Review, 139, 2399–2420, 2011.

Romatschke, U., Medina, S., and Houze Jr, R. A.: Regional, seasonal, and diurnal variations of extreme convection in the South Asian region, Journal of climate, 23, 419–439, 2010.

Rosenfeld, D.: TRMM observed first direct evidence of smoke from forest fires inhibiting rainfall, Geophysical research letters, 26, 3105–

260 3108, 1999.

Sátori, G., Williams, E., and Lemperger, I.: Variability of global lightning activity on the ENSO time scale, Atmospheric Research, 91, 500–507, 2009.

Schiemann, R., Lüthi, D., and Schär, C.: Seasonality and interannual variability of the westerly jet in the Tibetan Plateau region, Journal of Climate, 22, 2940–2957, 2009.

265 Selvi, S. and Rajapandian, S.: Analysis of lightning hazards in India, International Journal of Disaster Risk Reduction, 19, 22–24, 2016.

Singh, O. and Singh, J.: Lightning fatalities over India: 1979–2011, Meteorological Applications, 22, 770–778, 2015.

Syed, F., Giorgi, F., Pal, J., and King, M.: Effect of remote forcings on the winter precipitation of central southwest Asia part 1: observations, Theoretical and Applied Climatology, 86, 147–160, 2006.

Takahashi, T., Tajiri, T., and Sonoi, Y.: Charges on graupel and snow crystals and the electrical structure of winter thunderstorms, Journal of

270 the atmospheric sciences, 56, 1561–1578, 1999.

Tinmaker, M., Aslam, M., and Chate, D.: Lightning activity and its association with rainfall and convective available potential energy over Maharashtra, India, Natural Hazards, 77, 293–304, 2015.

Venevsky, S.: Importance of aerosols for annual lightning production at global scale., Atmospheric Chemistry & Physics, 14, 2014.

Williams, E., Rosenfeld, D., Madden, N., Gerlach, J., Gears, N., Atkinson, L., Dunnemann, N., Frostrom, G., Antonio, M., Biazon, B., et al.:

275 Contrasting convective regimes over the Amazon: Implications for cloud electrification, Journal of Geophysical Research: Atmospheres, 107, LBA–50, 2002.

Williams, E. R.: The Schumann resonance: A global tropical thermometer, Science, 256, 1184–1187, 1992.

Williams, E. R.: The electrification of severe storms, in: Severe Convective Storms, pp. 527–561, Springer, 2001.

Williams, E. R., Geotis, S., Renno, N., Rutledge, S., Rasmussen, E., and Rickenbach, T.: A radar and electrical study of tropical "hot towers",

280 Journal of the atmospheric sciences, 49, 1386–1395, 1992.

Yadava, P. K., Soni, M., Verma, S., Kumar, H., Sharma, A., and Payra, S.: The major lightning regions and associated casualties over India, Natural Hazards, 101, 217–229, 2020.

Yang, S., Lau, K., and Kim, K.: Variations of the East Asian jet stream and Asian–Pacific–American winter climate anomalies, Journal of Climate, 15, 306–325, 2002.

285 Zipser, E. J.: Deep cumulonimbus cloud systems in the tropics with and without lightning, Monthly weather review, 122, 1837–1851, 1994.

Zipser, E. J., Cecil, D. J., Liu, C., Nesbitt, S. W., and Yorty, D. P.: Where are the most intense thunderstorms on Earth?, Bulletin of the American Meteorological Society, 87, 1057–1072, 2006.

Zubair, L. and Ropelewski, C. F.: The strengthening relationship between ENSO and northeast monsoon rainfall over Sri Lanka and southern India, Journal of Climate, 19, 1567–1575, 2006.